View metadata, citation and similar papers at core.ac.uk

brought to you by CORE

provided by NASA Technical Reports Server

NASA TECHNICAL NOTE

NASA TN D-3099

c. 1

LOAN COPY: RETU
AFWL (WLIL
KIRTLAND AFB,

0130059

TECH LIBRARY KAFB, NM

NASA TN D-3099

ATTENUATION OF SINUSOIDAL PERTURBATIONS SUPERIMPOSED ON LAMINAR FLOW OF A LIQUID IN A LONG LINE

by Carl M. Holland, Robert J. Blade, and Robert G. Dorsch

Lewis Research Center
Cleveland, Ohio

RECEIVED
22 NOV 1965
Technical Library
AF Weapons Laboratory

NATIONAL AERONAUTICS AND SPACE ADMINISTRATION • WASHINGTON, D. C. • NOVEMBER 1965

TECH LIBRARY KAFB, NM
0130059

NASA TN D-3099

ATTENUATION OF SINUSOIDAL PERTURBATIONS SUPERIMPOSED ON LAMINAR FLOW OF A LIQUID IN A LONG LINE

By Carl M. Holland, Robert J. Blade, and Robert G. Dorsch

Lewis Research Center
Cleveland, Ohio

NATIONAL AERONAUTICS AND SPACE ADMINISTRATION

For sale by the Clearinghouse for Federal Scientific and Technical Information
Springfield, Virginia 22151 – Price $1.00

ATTENUATION OF SINUSOIDAL PERTURBATIONS SUPERIMPOSED ON LAMINAR FLOW OF A LIQUID IN A LONG LINE

by Carl M. Holland, Robert J. Blade, and Robert G. Dorsch

Lewis Research Center

SUMMARY

The attenuation constant for sinusoidal pressure and flow perturbations superimposed on the laminar flow of a viscous liquid was measured in a system consisting of a long, straight, cylindrical hydraulic line. The upstream and downstream ends of the line were securely fastened to the ground. A sinusoidal perturbation was imposed on the mean flow at the upstream end by means of a small oscillation of a throttle valve about a partly open mean position. The downstream end was terminated in a restricting orifice. Pressure perturbations were measured at three locations along the line for frequencies from 15 to 100 cps. These pressure measurements were reduced by use of a pair of complex damped acoustic one-dimensional wave equations to obtain the attenuation constant along with the phase constant and the dimensionless downstream admittance. For the range of frequencies investigated, the experimental values of the attenuation constant are in good agreement with classical theory.

INTRODUCTION

Acoustic pressure and flow perturbations in hydraulic lines are of importance in the operation of various fluid systems. The dynamics of hydraulic control and rocket-propellant feed systems are of particular interest to the aerospace industry. For example, longitudinal instability of liquid rocket boosters results from dynamic coupling between flow perturbations in the propellant feed system and structural oscillations. The Lewis Research Center has therefore conducted experimental and analytical studies of acoustic disturbances in flowing-liquid systems.

Transfer functions for acoustic disturbances superimposed on the turbulent flow of a liquid propellant flowing in long cylindrical lines of several geometrical networks are reported in references 1 to 3. These measurements were made with a nonviscous hydrocarbon liquid with small attenuation (about 3 percent per 100 ft). Other investigators have reported transfer functions and distributed line impedance for damped acoustic disturbances in lines containing a viscous liquid with appreciable attenuation (refs. 4 to 7).

The analytical expression for the pressure transfer function depends upon

three parameters: the attenuation constant, the phase constant, and the ratio of the downstream admittance to the characteristic admittance of the line (referred to herein as the "dimensionless downstream admittance"). Experimental values of the attenuation constant are reported in references 8 and 9 for sound waves in stationary air within tubes.

The results of an experimental study of the attenuation constant for acoustic disturbances superimposed on the mean laminar flow of a viscous liquid flowing in a long line are reported herein. Experimental data were obtained by measuring perturbation pressures at three stations along the line. Experimental values were computed from the data and compared with analytical values obtained from classical theory.

APPARATUS

Flow system. - The essential parts of the open-loop pumped-return flow system used in the experiment are shown in figure 1. The test fluid was an additive-free SAE 20 motor oil with a viscosity which resulted in laminar mean flow in the line at the operating conditions. The oil was supplied by a gear pump, and the mean flow rate was measured by means of a rotameter. A heat exchanger in the fluid-supply tank capable of either heating or cooling maintained the fluid at a constant temperature during each run. Hydraulic accumulators were placed between the pump and the test line to provide steady supply pressure. The discharge from the test line was submerged in a constant-height, vented tank. Fluid was returned to the supply tank by intermittent operation of the return pump.

Flow disturbance generator. - Sinusoidal perturbations of flow and pressure were induced in the system by means of an electrohydraulic servoactuated throttle located just upstream of the test line. The throttle was oscillated sinusoidally about a partly open mean position in response to an alternating voltage.

Test line. - The test line, made of stainless-steel tubing, 1.00 inch in outside diameter with a 0.065-inch wall thickness, was 68 feet long. A schematic diagram of the test line is shown in figure 2. The upstream end was attached to the throttle valve, which, in turn, was securely fastened to the ground. The downstream end was bolted to a 3-inch-diameter pipe fastened to a

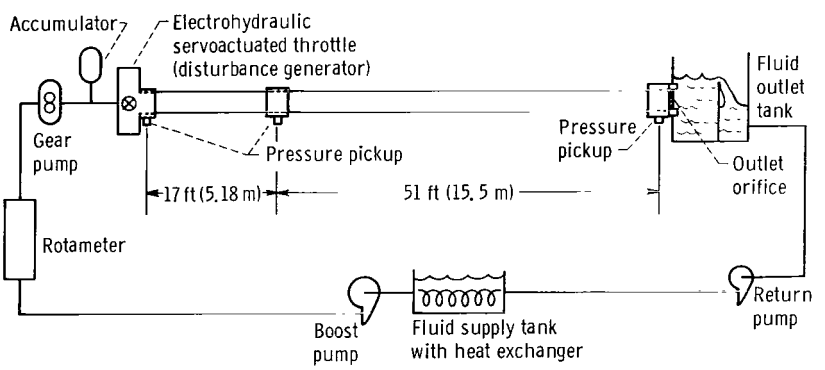

Figure 1. - Experimental setup of hydraulic lines.

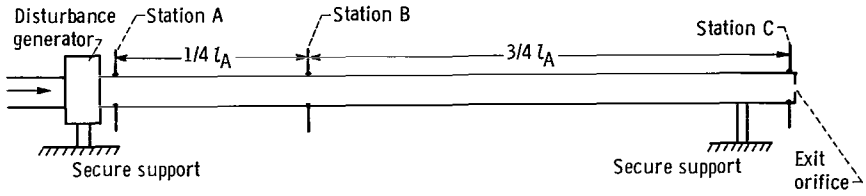

Figure 2. - Test line.

5-ton block of concrete set in the ground. Between the ends, the test line rested on horizontal transverse wires spaced at 2-foot intervals. The line was terminated in an orifice plate containing 21 holes, 0.040 inch in diameter. The orifice plate was rigidly attached to the line.

Instrumentation. - Pressure sensors, commercial flush diaphragm units, were rigidly attached to the line at stations A, B, and C (fig. 2). The pressure sensors with their associated amplifiers were calibrated by static methods. Relative gain factors among the sensors were then determined from the calibrations.

The output of the pressure sensors was in the form of alternating-current electrical signals with phase and amplitude determined by the local perturbation pressure. These alternating-current signals were amplified and fed into a transfer-function analyzer. The transfer-function analyzer consisted of two units: (1) an oscillator, which supplied (a) the signal to activate the electrohydraulic flow-disturbance generator and (b) a four-phase reference voltage to the resolved component indicator, and (2) a resolved component indicator, which indicated the in-phase and quadrature (90° out of phase) components of the pressure signals with respect to the reference voltage. The transfer-function analyzer effectively rejects all frequencies (associated with noise and harmonics) except the reference frequency (generated by the oscillator) and indicates the output signal of the pressure sensors in resolved component form.

PROCEDURE

Test. - The flow system was operated at constant mean flow rate, pressure, and temperature until conditions had stabilized. Mean gage pressure readings were taken at stations A and C, the mean flow rate was read on the rotameter, and the temperature adjacent to the downstream orifice was recorded. The servothrottle was operated at a series of frequencies. The amplitude of the throttle area variation was maintained constant over the entire range of frequencies for each run. It was kept small relative to the mean open area to avoid nonlinear effects but large enough to give an adequate ratio of signal to noise. The resulting average amplitude of sinusoidal pressure perturbations was about 15 pounds per square inch. At each frequency, the values of the in-phase and quadrature components of the three dynamic pressures (upstream, quarter length, and downstream) were read in succession on the resolved component indicator.

The mean pressure drop across the downstream orifice and the fluid temperature were constant during each run but were independently changed from run to run to vary the average orifice impedance (controlled by both of these factors) and the viscosity of the fluid (controlled mainly by fluid temperature).

The data were taken over a range of disturbance frequencies from 15 to 100 cps, mean line pressures from 165 to 315 pounds per square inch gage, and temperatures from 80° to 125° F. The range of variation of these parameters depended upon facility limitations. The range of frequencies, mean line pressures, and temperatures resulted in a range of absolute viscosities from 0.748×10^{-3} to 2.54×10^{-3} pound-second per square foot, Reynolds numbers of the mean flow (with inner tube diameter as the characteristic length) from 263 to 1200, mean flow rates from 5.5 to 8.0 feet per second, and magnitudes of dimensionless downstream admittance from 0.63 to 1.2.

The oil was deaerated between runs by flowing it at low speed and high temperature for about 1 hour through the receiving tank (fig. 1, p. 2) in which a vacuum of 10 inches of mercury existed. During each data run, the receiving tank was vented to the atmosphere.

Data analysis. - The following quantities were computed from the experimental data for each frequency:

(1) The attenuation constant α in nepers per foot

(2) The phase constant β in radians per foot

(3) The complex dimensionless admittance at station C, Z_o/Z_C

(All symbols are defined in appendix A.)

These quantities were computed from the data for each frequency by use of a pair of complex pressure transfer functions for (1) stations A and C (fig. 2) and (2) stations B and C. This pair of transfer functions is given by equations (1) and (2), respectively:

$$\frac{P_A}{P_C} = \cosh(\alpha + j\beta)l_A + \frac{Z_o}{Z_C} \sinh(\alpha + j\beta)l_A \qquad (1)$$

$$\frac{P_B}{P_C} = \cosh(\alpha + j\beta)l_B + \frac{Z_o}{Z_C} \sinh(\alpha + j\beta)l_B \qquad (2)$$

These equations were obtained from the well-known complex pressure transfer function for damped sinusoidal one-dimensional acoustic waves in uniform pipes. They were solved (see appendix B) on a digital computer by use of a numerical method.

The input data necessary were (1) the measured values of the in-phase and quadrature components of P_A, P_B, and P_C and (2) the distances in feet l_A and l_B between stations A and C and between stations B and C, respectively.

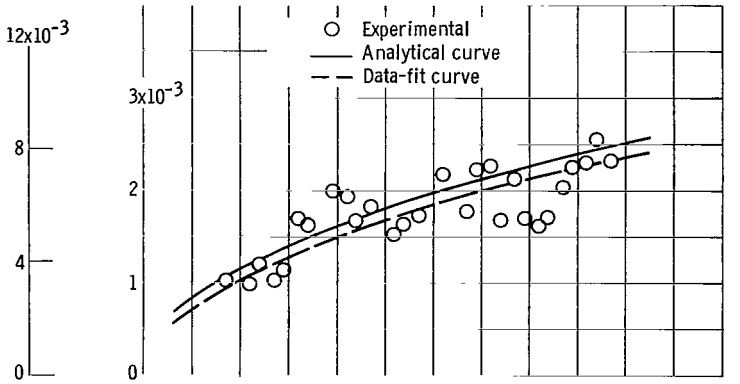

(a) Run a. Absolute viscosity of fluid, 0.748×10^{-3} pound-second per square foot (0.0358 N-sec/sq m); Reynolds number of mean flow, 1200.

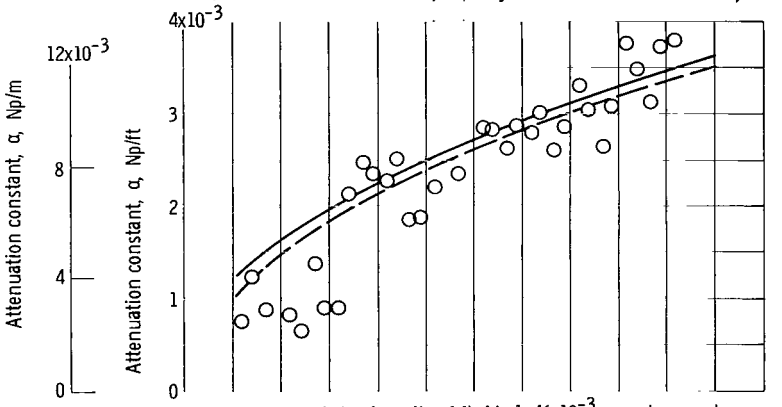

(b) Run b. Absolute viscosity of fluid, 1.46×10^{-3} pound-second per square foot (0.070 N-sec/sq m); Reynolds number of mean flow, 431.

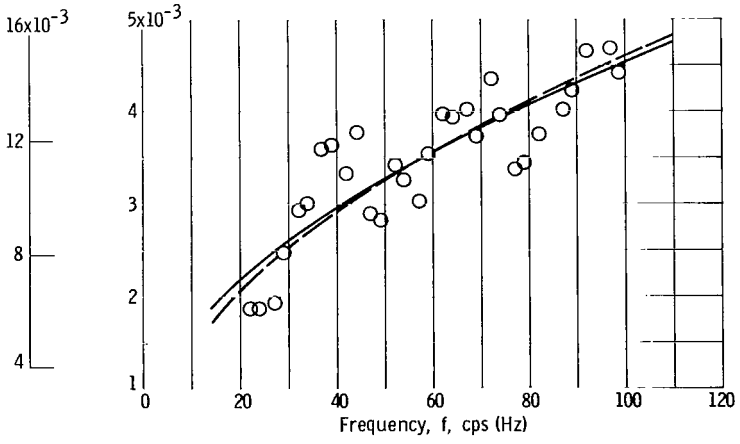

(c) Run c. Absolute viscosity of fluid, 2.54×10^{-3} pound-second per square foot (0.122 N-sec/sq m); Reynolds number of mean flow, 263.

Figure 3. - Variation of attenuation constant with frequency.

For comparison, theoretical values of the attenuation constant α, the phase constant β, and the specific characteristic impedance of the line Z_o were computed from classical equations derived in appendix C (primarily equations (C16), (C17), and (C18), respectively). The values of the density and the effective adiabatic bulk modulus of the liquid in the line required by these equations were obtained from the manufacturer and from references. (See appendix D for these values and references). The absolute viscosity in pound-seconds per square foot was obtained for each run from the mean-state data (mean pressures at stations A and C and mean flow rate) by use of Poiseuille's coefficient (ref. 10, p. 249).

RESULTS AND DISCUSSION

Experimental and analytical results for three runs (denoted herein as a, b, and c) that cover the range of mean line conditions are given in figures 3 to 5. The data points were calculated from experimental pressure measurements by the methods described in the PROCEDURE section and the analytical curves were obtained from the equations of appendix C.

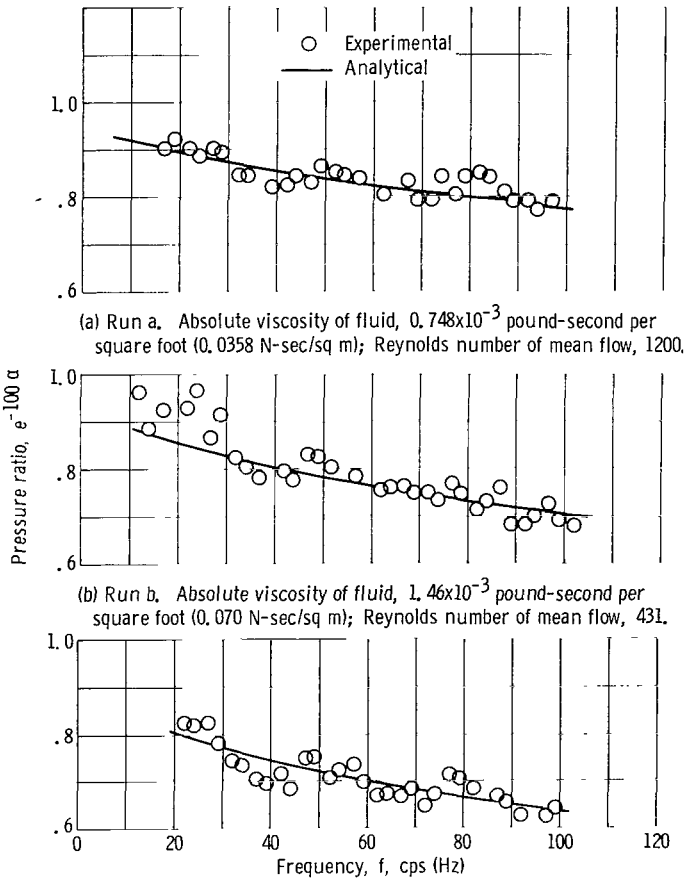

(a) Run a. Absolute viscosity of fluid, 0.748×10^{-3} pound-second per square foot (0.0358 N-sec/sq m); Reynolds number of mean flow, 1200.

(b) Run b. Absolute viscosity of fluid, 1.46×10^{-3} pound-second per square foot (0.070 N-sec/sq m); Reynolds number of mean flow, 431.

(c) Run c. Absolute viscosity of fluid, 2.54×10^{-3} pound-second per square foot (0.122 N-sec/sq m); Reynolds number of mean flow, 263.

Figure 4. - Effect of frequency on attenuation, expressed as pressure ratio $e^{-100\alpha}$, where α is attenuation constant.

Figure 3 gives the attenuation constant α in nepers per foot as a function of frequency. Dashed data-fit curves are shown along with the analytical curves and the data points. The data-fit curves were obtained by a least-squares method (appendix E) in which the attenuation constant was taken to be proportional to the square root of frequency. This functional relation was chosen for the data-fit curves because it is commonly used as an approximation (ref. 10, p. 242) to the exact analytical curve. Although there is considerable scatter in the individual data points, the data-fit and analytical curves are considered to agree within the limits of accuracy of the experiment.

As an illustration of the effect of the attenuation constant on acoustic disturbances traveling down the line, figure 4 presents the quantity $e^{-100\alpha}$ as a function of frequency. This quantity is the ratio of the amplitude of the

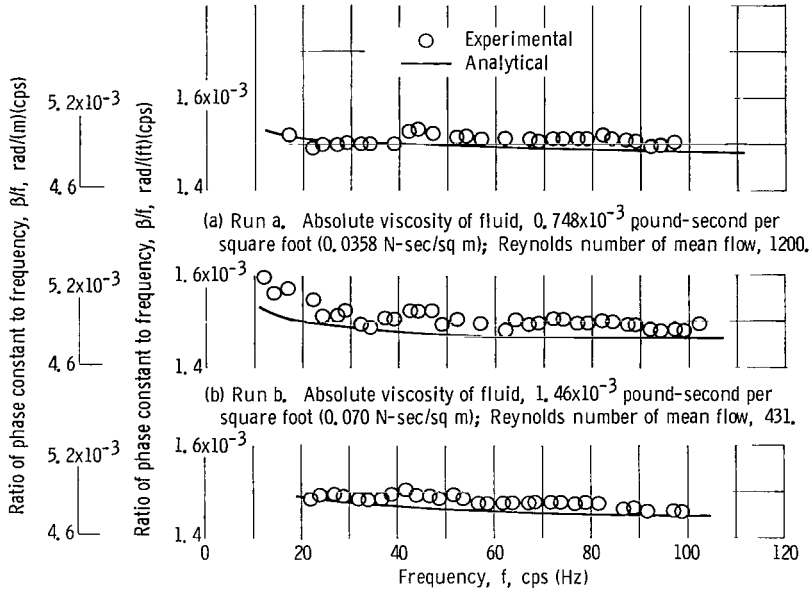

(a) Run a. Absolute viscosity of fluid, 0.748×10^{-3} pound-second per square foot (0.0358 N-sec/sq m); Reynolds number of mean flow, 1200.

(b) Run b. Absolute viscosity of fluid, 1.46×10^{-3} pound-second per square foot (0.070 N-sec/sq m); Reynolds number of mean flow, 431.

(c) Run c. Absolute viscosity of fluid, 2.54×10^{-3} pound-second per square foot (0.122 N-sec/sq m); Reynolds number of mean flow, 263.

Figure 5. - Effect of frequency on ratio of phase constant to frequency.

downstream to the upstream pressure perturbation for a wave traveling in the downstream direction for two points along a line which are separated by 100 feet (30.5 m). Figure 4 shows that for the conditions of this experiment the attenuation of pressure amplitude was of the order of 25 percent in a 100-foot line.

In addition to the attenuation constant, experimental and analytical values of the phase constant β (see eqs. (1) and (2)) were determined. These values are presented in figure 5 in the form β/f as a function of frequency. The experimental and analytical results are in good agreement. The quantity β/f is inversely proportional to the velocity of propagation of sinusoidal disturbance waves in the line c. More precisely,

$$\frac{\beta}{f} = \frac{2\pi}{c} \tag{3}$$

Figure 5 indicates that the value of the velocity of propagation was nearly constant for most frequencies of measurement.

As a check against obtaining extraneous roots in computing α, the experimental magnitude and angle of the complex dimensionless admittance at station C were compared with semianalytical values (see appendix B). These experimental and calculated values corresponding to the runs shown in figures 3 to 5 are given in table I. The mean experimental values of the magnitude of this ratio were in very good agreement with the calculated values; the maximum deviation of experiment from the calculations was less than ±11 percent. The maximum difference between the experimental and the calculated angles of this ratio was less than $\pm 10^{\circ}$. This agreement confirms the implied assumption that the method of computing the data gave the roots of interest.

TABLE I. - CALCULATED AND EXPERIMENTAL VALUES OF COMPLEX DOWNSTREAM DIMENSIONLESS ADMITTANCE Z_o/Z_c

Run a					Run b					Run c				
Frequency, cps	Magnitude of admittance Z_o/Z_c		Angle of admittance Z_o/Z_c, deg		Frequency, cps	Magnitude of admittance Z_o/Z_c		Angle of admittance Z_o/Z_c, deg		Frequency, cps	Magnitude of admittance Z_o/Z_c		Angle of admittance Z_o/Z_c, deg	
	Experimental	Calculated	Experimental	Calculated		Experimental	Calculated	Experimental	Calculated		Experimental	Calculated	Experimental	Calculated
17	0.65	0.67	0	-2	12	1.11	1.08	-7	-4	22	1.10	1.07	-2	-4
22	.65	.67	0	-2	14	1.08	1.08	-5	-4	24	1.08	1.07	-3	-4
24	.65	.67	0	-2	17	1.12	1.07	-6	-3	27	1.06	1.07	-1	-3
27	.64	.66	0	-2	22	1.12	1.07	-4	-3	29	1.04	1.07	-1	-3
29	.64	.66	0	-2	24	1.12	1.06	-2	-3	32	1.01	1.06	-1	-3
32	.63	.66	0	-2	27	1.07	1.06	-1	-3	34	1.00	1.06	-2	-3
34	.63	.66	1	-2	29	1.05	1.06	0	-3	37	.95	1.06	-4	-3
39	.64	.66	0	-2	32	1.00	1.06	2	-2	39	.96	1.06	-6	-3
42	.64	.66	-4	-1	34	1.01	1.06	0	-2	42	1.02	1.06	-10	-3
44	.66	.66	-5	-1	37	1.02	1.05	-1	-2	44	1.03	1.06	-8	-3
47	.67	.66	-3	-1	39	.95	1.05	-4	-2	47	1.08	1.05	-8	-3
52	.68	.66	1	-1	42	1.01	1.05	-10	-2	49	1.09	1.05	-6	-3
54	.69	.66	1	-1	44	.99	1.05	-9	-2	52	1.10	1.05	-5	-3
57	.67	.66	3	-1	47	1.05	1.05	-8	-2	54	1.10	1.05	-5	-3
62	.66	.66	3	-1	49	1.13	1.05	-3	-2	57	1.07	1.05	-4	-2
67	.66	.66	4	-1	52	1.10	1.05	-4	-2	59	1.07	1.05	-4	-2
69	.63	.66	4	-1	57	1.10	1.05	-3	-2	62	1.02	1.05	-3	-2
72	.63	.66	0	-1	62	.99	1.04	1	-2	64	1.05	1.05	-4	-2
74	.64	.66	1	-1	64	1.03	1.04	-3	-2	67	.99	1.05	-6	-2
77	.64	.66	-2	-1	67	1.02	1.04	-4	-2	69	1.00	1.05	-5	-2
79	.68	.66	-4	-1	69	1.00	1.04	-6	-2	72	1.00	1.05	-6	-2
82	.72	.66	-2	-1	72	1.03	1.04	-11	-2	74	1.00	1.05	-8	-2
84	.70	.66	1	-1	74	1.06	1.04	-9	-2	77	1.04	1.04	-7	-2
87	.71	.65	3	-1	77	1.05	1.04	-7	-2	79	1.11	1.04	-8	-2
89	.70	.65	7	-1	79	1.06	1.04	-7	-2	82	1.11	1.04	-5	-2
92	.69	.65	8	-1	82	1.08	1.04	-5	-2	84	1.04	1.04	-5	-2
94	.67	.65	7	-1	84	1.09	1.04	-5	-2	87	1.06	1.04	-4	-2
97	.68	.65	-4	-1	87	1.08	1.04	-4	-1	89	1.06	1.04	-5	-2
					89	1.06	1.04	-4	-1	92	1.06	1.04	-6	-2
					92	1.05	1.04	-6	-1	97	1.09	1.04	-7	-2
					94	1.03	1.04	-4	-1	99	1.09	1.04	-7	-2
					97	.99	1.04	-3	-1					
					99	.97	1.04	-6	-1					
					102	.95	1.04	-7	-1					

CONCLUSIONS

In a study of the attenuation of sinusoidal perturbations superimposed on laminar flow of a liquid in a long line, the experimental and analytical results were in good overall agreement. These results indicate that one-dimensional damped acoustic-wave theory, as presented herein, satisfactorily describes the attenuation constant and, more generally, sinusoidal disturbance propagation. This statement is restricted to laminar mean flow of viscous Newtonian liquids within long, firm-walled, nonvibrating, straight, cylindrical pipelines within the frequency range studied.

Lewis Research Center,
National Aeronautics and Space Administration,
Cleveland, Ohio, September 9, 1965.

APPENDIX A

SYMBOLS

A	constant defined by eq. (E4)
a	tube inner radius, ft (m)
c	velocity of sinusoidal wave propagation in line, ft/sec (m/sec)
f	frequency, cps (hertz)
I	defined by eq. (C10)
J_0	Bessel function of first kind of order zero
J_1	Bessel function of first kind of order one
j	$\sqrt{-1}$
K	effective adiabatic bulk modulus of liquid in line, lb/sq ft (N/m^2)
l	distance from station C (fig. 2), ft (m)
N	defined by eq. (C9)
n	number of data points in run
P	sinusoidal-disturbance complex pressure amplitude, P(x), lb/sq ft (N/m^2)
P_0	sinusoidal-disturbance complex pressure amplitude at x = 0 (station C) for component of wave that is traveling in negative x-direction, lb/sq ft (N/m^2)
p	disturbance pressure, p(x,t), lb/sq ft (N/m^2)
R	specific series resistance of line to sinusoidal perturbation, lb-sec/cu ft ($N\text{-sec}/m^3$)
Re	Reynolds number of mean flow with use of inner tube diameter as characteristic length
r	radial coordinate in any cross-sectional plane of line with r = 0 along axis, ft (m)
t	time, sec
U	complex amplitude of sinusoidal-perturbation velocity in x-direction averaged over cross-sectional area of line, U(x), ft/sec (m/sec)

$U'(x,r)$ complex amplitude of sinusoidal-perturbation velocity in x-direction, ft/sec (m/sec)

u perturbation velocity in x-direction averaged over cross-sectional area of line, $u(x,t)$, ft/sec (m/sec)

u' perturbation velocity in x-direction, $u'(x,r,t)$, ft/sec (m/sec)

v' perturbation velocity in r-direction, $v'(x,r,t)$, ft/sec (m/sec)

x coordinate in axial direction of line with $x = 0$ at station C (fig. 2) and positive direction in upstream direction, ft (m)

Z_C specific impedance at station C (fig. 2) looking downstream, a complex number (approximately real in this experiment), lb-sec/cu ft (N-sec/m^3)

Z_o specific characteristic impedance of line, a complex number, lb-sec/cu ft (N-sec/m^3)

α attenuation constant, Np/ft (Np/m)

β phase constant, rad/ft (rad/m)

μ absolute viscosity of fluid, lb-sec/sq ft (N-sec/m^2)

ρ density of fluid (denotes mean value except in $\partial\rho$), slugs/cu ft (kg/m^3)

ρ_e effective density of fluid defined by eq. (C12), slugs/cu ft (kg/m^3)

ω frequency, $2\pi f$, rad/sec

Subscripts:

A station A (fig. 2)

B station B (fig. 2)

C station C (fig. 2)

F data fit

i data point

x real part of complex number

y imaginary part (quadrature component) of complex number

APPENDIX B

DETERMINATION OF PRESSURE TRANSFER FUNCTION PARAMETERS FROM DATA

Using identities and equating the real and the imaginary components of equations (1) and (2) gives four equations in the four unknowns α, β, $(Z_o/Z_C)_x$, and $(Z_o/Z_C)_y$ as follows:

$$\left(\frac{P_A}{P_C}\right)_x = (\cosh \alpha l_A)\cos \beta l_A + \left(\frac{Z_o}{Z_C}\right)_x (\sinh \alpha l_A)\cos \beta l_A - \left(\frac{Z_o}{Z_C}\right)_y (\cosh \alpha l_A)\sin \beta l_A \tag{B1}$$

$$\left(\frac{P_A}{P_C}\right)_y = (\sinh \alpha l_A)\sin \beta l_A + \left(\frac{Z_o}{Z_C}\right)_x (\cosh \alpha l_A)\sin \beta l_A + \left(\frac{Z_o}{Z_C}\right)_y (\sinh \alpha l_A)\cos \beta l_A \tag{B2}$$

$$\left(\frac{P_B}{P_C}\right)_x = (\cosh \alpha l_B)\cos \beta l_B + \left(\frac{Z_o}{Z_C}\right)_x (\sinh \alpha l_B)\cos \beta l_B - \left(\frac{Z_o}{Z_C}\right)_y (\cosh \alpha l_B)\sin \beta l_B \tag{B3}$$

$$\left(\frac{P_B}{P_C}\right)_y = (\sinh \alpha l_B)\sin \beta l_B + \left(\frac{Z_o}{Z_C}\right)_x (\cosh \alpha l_B)\sin \beta l_B + \left(\frac{Z_o}{Z_C}\right)_y (\sinh \alpha l_B)\cos \beta l_B \tag{B4}$$

Eliminating $(Z_o/Z_C)_x$ and $(Z_o/Z_C)_y$ from equations (B1) to (B4) and using identities gives two equations in the two unknowns α and β:

$$\begin{vmatrix} (\sinh \alpha l_A)\cos \beta l_A & \left(\frac{P_A}{P_C}\right)_x \\ (\sinh \alpha l_B)\cos \beta l_B & \left(\frac{P_B}{P_C}\right)_x \end{vmatrix} - \begin{vmatrix} (\cosh \alpha l_A)\sin \beta l_A & \left(\frac{P_A}{P_C}\right)_y \\ (\cosh \alpha l_B)\sin \beta l_B & \left(\frac{P_B}{P_C}\right)_y \end{vmatrix}$$

$$- [\sinh \alpha(l_A - l_B)]\cos \beta(l_A - l_B) = 0 \tag{B5}$$

$$\begin{vmatrix} \left(\frac{P_A}{P_C}\right)_x & -(\cosh \alpha l_A)\sin \beta l_A \\ \left(\frac{P_B}{P_C}\right)_x & -(\cosh \alpha l_B)\sin \beta l_B \end{vmatrix} - \begin{vmatrix} \left(\frac{P_A}{P_C}\right)_y & (\sinh \alpha l_A)\cos \beta l_A \\ \left(\frac{P_B}{P_C}\right)_y & (\sinh \alpha l_B)\cos \beta l_B \end{vmatrix}$$

$$-[\sin \beta(l_A - l_B)]\cosh \alpha(l_A - l_B) = 0 \qquad \text{(B6)}$$

Equations (B5) and (B6) were solved for α and β on a digital computer by use of a numerical solution, the Newton-Raphson method. The criterion of convergence both α and β were forced to satisfy was that the magnitude of (1) the difference between two successive values of the unknown (α,β) computed by the numerical method for a given frequency divided by (2) the last computed value of the unknown at that frequency must be less than or equal to 5×10^{-6}. Initial estimates for α and β were made for the calculation at the highest frequency of each run. The values to which α and β converged at a given frequency were used as the initial estimate in the numerical solution at the next lower frequency of measurement.

The unknowns $(Z_o/Z_C)_x$ and $(Z_o/Z_C)_y$ can be calculated as follows: Equations (B1) and (B2) give

$$\left(\frac{Z_o}{Z_C}\right)_y = \left[\left(\frac{P_A}{P_C}\right)_y (\sinh \alpha l_A)\cos \beta l_A - \left(\frac{P_A}{P_C}\right)_x (\cosh \alpha l_A)\sin \beta l_A + (\cos \beta l_A)\sin \beta l_A\right]\left[(\cosh^2\alpha l_A)\sin^2\beta l_A + (\sinh^2\alpha l_A)\cos^2\beta l_A\right]^{-1} \qquad \text{(B7)}$$

and

$$\left(\frac{Z_o}{Z_C}\right)_x = \left[\left(\frac{P_A}{P_C}\right)_y (\sin \beta l_A)\cosh \alpha l_A + \left(\frac{P_A}{P_C}\right)_x (\cos \beta l_A)\sinh \alpha l_A - (\sinh \alpha l_A)\cosh \alpha l_A\right]\left[(\cosh^2\alpha l_A)\sin^2\beta l_A + (\sinh^2\alpha l_A)\cos^2\beta l_A\right]^{-1} \qquad \text{(B8)}$$

The values of $(Z_o/Z_C)_x$ and $(Z_o/Z_C)_y$ were computed for each frequency by substituting the values of α and β, obtained from the numerical solution of equations (B5) and (B6), into equations (B7) and (B8). Note that the experimental values of $(P_A/P_C)_x$ and $(P_A/P_C)_y$ are explicitly required in equations (B7) and (B8).

As a check against obtaining extraneous roots in computing α, the experimental magnitude and angle of the complex dimensionless admittance at station C were compared with values obtained from (1) an equation for the specific characteristic impedance of the line (eq. (C18)) and (2) an approximation of the specific impedance at station C looking downstream (fig. 2) obtained by taking it as the resistance of the downstream orifice found from the slope of a curve of mean pressure against fluid velocity. These experimental and calculated values corresponding to the runs shown in figures 3 to 5 are given in table I (p. 8).

APPENDIX C

DERIVATION OF ANALYTICAL PRESSURE TRANSFER FUNCTION AND RELATED PARAMETERS FOR SMALL SINUSOIDAL PERTURBATIONS SUPERIMPOSED ON MEAN LAMINAR FLOW

Assumptions

The following assumptions lead to a system of partial differential equations:

(1) The fluid was considered Newtonian.

(2) Stokes hypothesis (ref. 11, p. 383) was assumed to apply.

(3) The medium was continuous and uniform.

(4) The absolute viscosity was considered constant.

(5) Axial symmetry was assumed to exist, because the line was cylindrical and its axis was straight.

(6) The perturbation flow was regarded as laminar.

(7) The viscous force that is proportional to $\partial^2 u'/\partial x^2$ (ref. 5) and end effects were neglected, because the ratio of tube inner radius to line length was small, 6.1×10^{-4}.

(8) The pressure across the cross section of the fluid can be considered constant, because of (a) the existing condition $\mu/a\sqrt{\rho K} \ll 1$ (ref. 7), (b) the rigidity of the pipe walls (ref. 6), and (c) the straightness of the pipe.

(9) The nonlinear convective acceleration terms in the momentum equation were neglected, because the ratio of mean flow speed to the velocity of sinusoidal-disturbance wave propagation was small, less than 5×10^{-3} (ref. 5).

(10) The change of density with position at any instant can be neglected, because the adiabatic bulk modulus of the liquid in the line was at least 3.0×10^7 pounds per square foot (ref. 5).

(11) The energy equation had little effect on the solution, because (a) heat conduction can be ignored because of the small difference between the ratio of specific heats and 1 (0.159) and the large Prandtl number (about 28) (refs. 10, p. 243, and 7) and (b) heat radiation can be ignored.

(12) The classical thermodynamic equation of state was used, because attenuation due to molecular exchanges of energy (discussed in ref. 11) was assumed negligible.

Basic Equations

It follows from the assumptions that the system is described by three partial differential equations (ref. 5). The momentum equation is

$$-\frac{\partial p}{\partial x} = \rho \frac{\partial u'}{\partial t} - \frac{\mu}{r} \frac{\partial}{\partial r}\left(r \frac{\partial u'}{\partial r}\right) \tag{C1}$$

The continuity equation is

$$\frac{\partial \rho}{\partial t} + \rho \frac{\partial v'}{\partial r} + \rho \frac{v'}{r} + \rho \frac{\partial u'}{\partial x} = 0 \tag{C2}$$

The thermodynamic equation of state for a liquid is

$$\frac{\partial \rho}{\rho} = \frac{\partial p}{K} \tag{C3}$$

Combining equations (C2) and (C3) and averaging the result over the cross-sectional area of the line gives (ref. 5)

$$\frac{\partial p}{\partial t} = -K \frac{\partial u}{\partial x} \tag{C4}$$

The steady-state solution only is sought. For a sinusoidal disturbance, the perturbation velocity in the axial direction u' and the perturbation pressure p can be written as

$$u' = U'(x,r)e^{j\omega t} \tag{C5}$$

$$p = Pe^{j\omega t} \tag{C6}$$

where P is a function of x only. For a tube wall that is stationary in the axial direction, the component of fluid velocity in the axial direction at the wall of the tube is zero. Therefore,

$$U'(x,a) = 0 \tag{C7}$$

Substituting equations (C5) and (C6) into equation (C1), solving for $U'(x,r)$ with the use of equation (C7), and averaging the resulting equation over a cross-sectional area gives the complex amplitude of the velocity perturbation averaged over a cross-sectional area as (ref. 10, p. 240)

$$U = \frac{\frac{\partial P}{\partial x}}{\mu N^2}\left(1 - \frac{2}{aN}\frac{J_1(aN)}{J_0(aN)}\right) \tag{C8}$$

where

$$N = (1 - j)\sqrt{\frac{\rho\omega}{2\mu}} \tag{C9}$$

Define

$$I = \frac{2}{a}\frac{J_1(aN)}{J_0(aN)} \tag{C10}$$

Rearranging equation (C8) gives

$$-\frac{\partial P}{\partial x} = (R + j\omega\rho_e)U \tag{C11}$$

where the effective density of the fluid (also referred to as the "distributed specific series inertance") is

$$\rho_e = \frac{\rho\sqrt{\frac{\rho\omega}{2\mu}}\left(2\sqrt{\frac{\rho\omega}{2\mu}} + I_y - I_x\right)}{\left(\sqrt{\frac{\rho\omega}{2\mu}} - I_x\right)^2 + \left(\sqrt{\frac{\rho\omega}{2\mu}} + I_y\right)^2} \tag{C12}$$

and the distributed specific series resistance is

$$R = \frac{-\rho\omega\sqrt{\frac{\rho\omega}{2\mu}}\,(I_x + I_y)}{\left(\sqrt{\frac{\rho\omega}{2\mu}} - I_x\right)^2 + \left(\sqrt{\frac{\rho\omega}{2\mu}} + I_y\right)^2} \tag{C13}$$

Generally following the method of reference 10 (pp. 233-236), that is, solving equations (C4) (with the use of complex notation) and (C11) for P and U and using the boundary condition

$$\frac{P_C}{U_C} = Z_C \quad \text{at} \quad x = 0 \text{ (station C)} \tag{C14}$$

gives

$$P = 2P_O\,\frac{Z_C\cosh(\alpha + j\beta)x + Z_O\sinh(\alpha + j\beta)x}{Z_O + Z_C} \tag{C15}$$

where the attenuation constant is the positive root of

$$\alpha = \left[\frac{\omega}{2K}\left(\sqrt{\omega^2\rho_e^2 + R^2} - \omega\rho_e\right)\right]^{1/2} \tag{C16}$$

the phase constant is

$$\beta = \sqrt{\omega^2\frac{\rho_e}{K} + \alpha^2} \tag{C17}$$

the specific characteristic impedance of the line is

$$Z_o = \frac{K}{\omega}(\beta - j\alpha) \tag{C18}$$

and P_0 is a constant. (Physically, P_0 is the disturbance complex pressure amplitude at $x = 0$ for the component of the wave that is traveling in the negative x-direction.)

Transfer Function

From equation (C15) the complex amplitude of the pressure perturbation at station C ($x = 0$) is

$$P_C = 2P_0 \frac{Z_C}{Z_o + Z_C} \tag{C19}$$

Dividing equation (C15) by equation (C19) gives

$$\frac{P}{P_C} = \cosh(\alpha + j\beta)x + \frac{Z_o}{Z_C}\sinh(\alpha + j\beta)x \tag{C20}$$

from which equations (1) and (2) immediately follow.

Calculation of Parameters

In order to calculate the theoretical values of α, β, and Z_o, I_x and I_y must be found. It is noted that

$$N = -\sqrt{\frac{\rho\omega}{\mu}}\, j^{3/2} \tag{C21}$$

Equation (C21) and the definition of Bessel-Kelvin functions of the first kind given in reference 12 yield

$$J_0(aN) = \mathrm{ber}_0\left(-a\sqrt{\frac{\rho\omega}{\mu}}\right) + j\,\mathrm{bei}_0\left(-a\sqrt{\frac{\rho\omega}{\mu}}\right) \tag{C22}$$

and

$$J_1(aN) = \mathrm{ber}_1\left(-a\sqrt{\frac{\rho\omega}{\mu}}\right) + j\,\mathrm{bei}_1\left(-a\sqrt{\frac{\rho\omega}{\mu}}\right) \tag{C23}$$

where $\mathrm{ber}_0(-a\sqrt{\rho\omega/\mu})$, $\mathrm{bei}_0(-a\sqrt{\rho\omega/\mu})$, $\mathrm{ber}_1(-a\sqrt{\rho\omega/\mu})$, and $\mathrm{bei}_1(-a\sqrt{\rho\omega/\mu})$ are real. Tables (refs. 12 and 13) do not explicitly give values of ber_1 and bei_1. They can be evaluated from the relations (ref. 13)

$$\mathrm{ber}_1 = \frac{1}{\sqrt{2}}(\mathrm{ber}_0' - \mathrm{bei}_0') \tag{C24}$$

and

$$\text{bei}_1 = \frac{1}{\sqrt{2}} (\text{ber}_0' + \text{bei}_0') \tag{C25}$$

Series forms of ber_0, bei_0, ber_0', and bei_0', given in reference 12, and equations (C22) to (C25) yield

$$J_0(aN) = \text{ber}_0 \left(a\sqrt{\frac{\rho\omega}{\mu}}\right) + j\text{bei}_0 \left(a\sqrt{\frac{\rho\omega}{\mu}}\right) \tag{C26}$$

$$J_1(aN) = -\text{ber}_1 \left(a\sqrt{\frac{\rho\omega}{\mu}}\right) - j\text{bei}_1 \left(a\sqrt{\frac{\rho\omega}{\mu}}\right) \tag{C27}$$

Combining equations (C10), (C26), and (C27) and rearranging terms gives

$$I_x = -\frac{2}{a} \frac{\text{ber}_1 \left(a\sqrt{\frac{\rho\omega}{\mu}}\right)\text{ber}_0 \left(a\sqrt{\frac{\rho\omega}{\mu}}\right) + \text{bei}_1 \left(a\sqrt{\frac{\rho\omega}{\mu}}\right)\text{bei}_0 \left(a\sqrt{\frac{\rho\omega}{\mu}}\right)}{\text{ber}_0^2 \left(a\sqrt{\frac{\rho\omega}{\mu}}\right) + \text{bei}_0^2 \left(a\sqrt{\frac{\rho\omega}{\mu}}\right)} \tag{C28}$$

$$I_y = \frac{2}{a} \frac{\text{ber}_1 \left(a\sqrt{\frac{\rho\omega}{\mu}}\right)\text{bei}_0 \left(a\sqrt{\frac{\rho\omega}{\mu}}\right) - \text{bei}_1 \left(a\sqrt{\frac{\rho\omega}{\mu}}\right)\text{ber}_0 \left(a\sqrt{\frac{\rho\omega}{\mu}}\right)}{\text{ber}_0^2 \left(a\sqrt{\frac{\rho\omega}{\mu}}\right) + \text{bei}_0^2 \left(a\sqrt{\frac{\rho\omega}{\mu}}\right)} \tag{C29}$$

The values of α, β, and Z_o can now be obtained for a given frequency from tables (refs. 12 and 13) and the appropriate preceding equations.

Simpler approximate formulas for the attenuation constant α, the phase constant β, and the specific characteristic impedance of the line Z_o are given in references 7 and 10.

APPENDIX D

PHYSICAL CONSTANTS OF TEST OIL

The values of the density ρ of the test oil were obtained from the manufacturer. All other physical constants were obtained from references 14 and 15 for an oil of the same density and viscosity as those of the test oil. The minimum Prandtl number for the oil in the tests was 28; the ratio of specific heats in the experiment was 1.159. The density and bulk modulus of the oil are given in the following table:

Run	Temperature		Density		Adiabatic bulk modulus[a]	
	^{o}F	^{o}K	slugs/cu ft	kg/cu m	lb/sq ft	N/sq m
a	125	325	1.65	850	3.04×10^{7}	1.46×10^{9}
b	100	311	1.67	861	3.22	1.54
c	80	300	1.68	866	3.37	1.61

[a]Corrected for line compliance as in ref. 1.

APPENDIX E

DETERMINATION OF BEST CURVE THROUGH EXPERIMENTAL ATTENUATION CONSTANT DATA POINTS

A best-fit curve of the form

$$\alpha_F = A\sqrt{f} \tag{E1}$$

is determined by a least-squares method. The constant A is chosen such that

$$\sum_i^n \left(\alpha_i - A\sqrt{f_i}\right)^2 = \text{Minimum} \tag{E2}$$

Equation (E2) requires

$$\sum_i^n \left(\alpha_i - A\sqrt{f_i}\right)\sqrt{f_i} = 0 \tag{E3}$$

Solving equation (E3) for the desired value of A gives

$$A = \frac{\sum_i^n \alpha_i \sqrt{f_i}}{\sum_i^n f_i} \tag{E4}$$

REFERENCES

1. Regetz, John D., Jr.: An Experimental Determination of the Dynamic Response of a Long Hydraulic Line. NASA TN D-576, 1960.

2. Blade, Robert J.; Lewis, William; and Goodykoontz, Jack H.: Study of a Sinusoidally Perturbed Flow in a Line Including a 90° Elbow with Flexible Supports. NASA TN D-1216, 1962.

3. Lewis, William; Blade, Robert J.; and Dorsch, Robert G.: Study of the Effect of a Closed-End Side Branch on Sinusoidally Perturbed Flow of Liquid in a Line. NASA TN D-1876, 1963.

4. Thurston, George B.: Periodic Fluid Flow Through Circular Tubes. J. Acoust. Soc. Am., vol. 24, no. 6, Nov. 1952, pp. 653-656.

5. D'Souza, Anthony Frank: Dynamic Response of Fluid Flow Through Straight and Curved Lines. Ph.D. Thesis, Purdue Univ., 1963.

6. Goodson, Raymond Eugene: Viscous and Boundary Effects in Fluid Lines. Ph.D. Thesis, Purdue Univ., 1963.

7. Brown, F. T.: The Transient Response of Fluid Lines. J. Basic Eng. (Trans. ASME), ser. D, vol. 84, no. 4, Dec. 1962, pp. 547-553.

8. Fay, R. D.: Attenuation of Sound in Tubes. J. Acoust. Soc. Am., vol. 12, no. 1, July 1940, pp. 62-67.

9. Fisher, R. C.: Theory of Sound Transmission in a Cylindrical Tube Filled with Viscous Fluid. Document No. D-18142, Boeing Airplane Co., Mar. 6, 1957.

10. Kinsler, Lawrence E.; and Frey, Austin R.: Fundamentals of Acoustics. First ed., John Wiley & Sons, Inc., 1950.

11. Markham, Jordan J.; Beyer, Robert T.; and Lindsay, R. B.: Absorption of Sound in Fluids. Rev. Modern Phys., vol. 23, no. 4, Oct. 1951, pp. 353-411.

12. Lowell, Herman, H.: Tables of the Bessel-Kelvin Functions ber, bei, ker, kei, and Their Derivatives for the Argument Range 0(0.01)107.50. NASA TR R-32, 1959.

13. Nosova, L. N. (Prasenijit Basu, trans.): Tables of Thomson Functions and Their First Derivatives. Pergamon Press, 1961.

14. Jessup, R. S.: Compressibility and Thermal Expansion of Petroleum Oils in the Range 0° to 300° C. J. Res. Nat. Bur. Standards, vol. 5, no. 5, Nov. 1930, pp. 985-1011.

15. Cragoe, C. S.: Thermal Properties of Petroleum Products. Misc. Publ. No. 97, NBS, 1929.

3/18/85

"The aeronautical and space activities of the United States shall be conducted so as to contribute . . . to the expansion of human knowledge of phenomena in the atmosphere and space. The Administration shall provide for the widest practicable and appropriate dissemination of information concerning its activities and the results thereof."

—NATIONAL AERONAUTICS AND SPACE ACT OF 1958

NASA SCIENTIFIC AND TECHNICAL PUBLICATIONS

TECHNICAL REPORTS: Scientific and technical information considered important, complete, and a lasting contribution to existing knowledge.

TECHNICAL NOTES: Information less broad in scope but nevertheless of importance as a contribution to existing knowledge.

TECHNICAL MEMORANDUMS: Information receiving limited distribution because of preliminary data, security classification, or other reasons.

CONTRACTOR REPORTS: Technical information generated in connection with a NASA contract or grant and released under NASA auspices.

TECHNICAL TRANSLATIONS: Information published in a foreign language considered to merit NASA distribution in English.

TECHNICAL REPRINTS: Information derived from NASA activities and initially published in the form of journal articles.

SPECIAL PUBLICATIONS: Information derived from or of value to NASA activities but not necessarily reporting the results of individual NASA-programmed scientific efforts. Publications include conference proceedings, monographs, data compilations, handbooks, sourcebooks, and special bibliographies.

Details on the availability of these publications may be obtained from:

SCIENTIFIC AND TECHNICAL INFORMATION DIVISION

NATIONAL AERONAUTICS AND SPACE ADMINISTRATION

Washington, D.C. 20546